Radiation Field of a Conical Helix

J. S. Chatterjee

Citation: J. Appl. Phys. **24**, 550 (1953); doi: 10.1063/1.1721328
View online: http://dx.doi.org/10.1063/1.1721328
View Table of Contents: http://jap.aip.org/resource/1/JAPIAU/v24/i5
Published by the American Institute of Physics.

in Fig. 3. The integral in Eq. (24) can be reduced to real integrals, and actual integration carried out numerically. Care must be taken to maintain the proper phase of the radicals.

An interesting check of the solution can be obtained by letting $a=0$, $b>0$ in either the transform solution or the far field solution. This is the situation for which the current element lies on the surface of the conductor. Now the branch point at $\gamma=-j\beta$ is no longer present, and the path of integration can be closed at infinity to the left. Evaluation by the theory of residues shows the field to be everywhere zero, which is the expected result.

The far field pattern given by Eq. (23) is also the pattern of a stub antenna (or finite length line source) in the plane perpendicular to its axis. That this is so can be seen as follows. The far field from an infinite line source is characterized mathematically by the assumption that each differential element of length sees the field point at right angles to its axis. Thus, by superposition, the pattern is also that from a single differential dipole, in the plane perpendicular to its axis.

A pattern has been calculated by numerical integration for the case where the source was a distance $\lambda/4$ from the plane reflector and $\lambda/4$ back from the edge, that is, $\beta a=\lambda/4$, $\beta b=\lambda/4$. Experimental measurements were taken on a model for the same conditions, using a stub antenna for the source. The results are given in Fig. 4. The experimental and theoretical patterns are in good agreement within the experimental accuracy.

JOURNAL OF APPLIED PHYSICS VOLUME 24, NUMBER 5 MAY, 1953

Radiation Field of a Conical Helix

J. S. CHATTERJEE
Institute of Radio Physics and Electronics, Calcutta University, Calcutta, India
(Received November 5, 1952)

It is now well known that a cylindrical helix, when excited at frequencies corresponding to wavelengths comparable to the length of one turn of the helix, can radiate a sharp beam along the axis over a wide frequency range (about one octave). It is shown in the present communication that if the helix be conical instead of cylindrical (the diameter varying along the length of helix), then the axial mode of radiation can be maintained over a much wider band of frequencies. The radiation pattern of a conical helix, 60 cm diameter at the base, tapering linearly to 20 cm at the top in 10 turns within a height of 112 cm (with the "ground" provided by brass disk of 100 cm in diameter) has been studied experimentally. It is found that the axial mode of radiation is maintained from 150 Mc/sec to 450 Mc/sec. By increasing the number of turns, the band width can be considerably increased. Assuming a linear current distribution, theoretical expressions have also been deduced for E_ϕ and E_θ for a conical helix. Some modifications of the simple conical helix, such as may have special applications, are indicated.

I. INTRODUCTION

A CYLINDRICAL helix is a well-known circuit element having many uses. It is widely used, for example, as an inductance; in a traveling wave tube it is used to guide the wave along the axis with a velocity smaller than that of light. In all such applications, the helix diameter is a small fraction of the free space wavelength corresponding to the frequencies concerned. Uses have also been found in recent years of a helix, the diameter of which is of the same order as the free space wavelength. It has been shown by Kraus[1] that for such wavelengths, the circular helix can be an efficient radiator. Depending upon the pitch angle and upon the ratio of the wavelength to the helix diameter, the helix can radiate in three modes. For example, for the pitch angle of 12.6° the so-called "normal" radiation mode (resulting from the T_0 mode of current) is observed when the length of one turn of the helix is smaller than 0.8λ; when this length is between $0.8\lambda-1.3\lambda$, the "axial" radiation mode, due to the T_1 mode of current distribution along the helix, is obtained; and, when the length is more than 1.3λ, energy is radiated in the "conical" mode due also to T_2 mode of current distribution.[2,3] Further, for the axial mode of radiation, a sharp beam is maintained along the axis over the large frequency band of nearly one octave. The three modes[2] of radiation are illustrated in Fig. 1.

It is interesting to inquire how the radiation characteristic of the helix will be altered, if the diameter instead of remaining constant varies along the length of the helix. This problem has been investigated both experimentally and theoretically by the author of the paper for the case of a simple conical helix, the radius of which varies along the length of the axis and the pitch angle remaining constant. It has been found that for such a helix there exists in general all the three modes of radiation as in the case of the cylindrical helix. The normal radiation mode is present when the frequency is

[1] J. D. Kraus, Electronics **20**, No. 4, 109 (1947).

[2] J. D. Kraus and J. C. Williamson, J. Appl. Phys. **19**, 87 (1948).
[3] J. A. Marsh, Proc. Inst. Radio Engrs. **39**, 668 (1951).

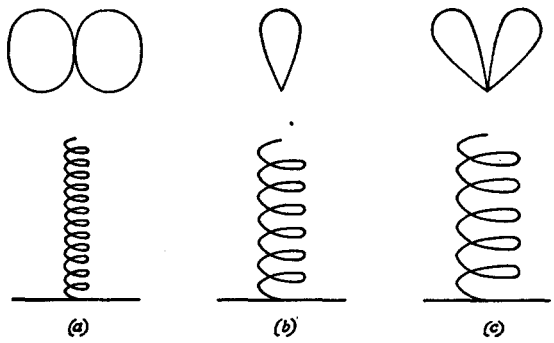

FIG. 1. Three types of radiation pattern of a cylindrical helix: (a) normal mode, (b) axial mode, (c) conical mode.

so low that at no part of the helix the diameter is large enough to satisfy the condition of axial mode of radiation. The axial mode is obtained with higher frequencies. In the transition range of frequencies, the portion of the helix having smaller diameter radiates in the normal mode; of the rest, the part having the larger and the appropriate diameter radiates in the axial mode. At still higher frequencies, the diameter at some portion of the helix becomes large enough (compared to the free space wavelength) for the conical mode of radiation to appear. The relative strengths of these three modes of radiation depend on the frequency and on the position of the point at which energy is introduced for exciting the helical antenna. This is because the feed position determines the current strengths in the different parts of the helix. For example, with the helix used by us for 450 Mc/sec, the radiation is mainly in the axial mode for the "apex feed," the conical mode of radiation just appearing. For the "base feed" the conical mode of radiation is stronger than the axial mode at 400 Mc/sec. Besides other interesting properties, the conical helix can radiate efficiently a beam of small angle over a frequency range which is much greater than that for the corresponding cylindrical helix.

In what follows we shall first describe the results of experimental investigation on the polar diagrams and on the charge distributions along a conical helix of chosen dimensions when it is excited to radiate the different modes. An attempt will then be made to develop a theory of radiation from such a simple conical antenna (Sec. III). Modification of the simple conical helical form to meet the demands of special applications will also be briefly indicated (Sec. IV).

II. EXPERIMENTS WITH A CONICAL HELIX

The form of a simple conical helix can be expressed in cylindrical coordinates (z, a, ϕ) by the equations,

$$a=a_0(1-k\phi) \tag{1}$$

and

$$dz=a\tan\alpha\cdot d\phi, \tag{2}$$

where a is the distance of an element of the helix from the axis.

$$z=\int_0^{\phi} a_0(1-k\phi)\tan\alpha\cdot d\phi=a_0\tan\alpha\left(1-\frac{k\phi}{2}\right)\phi, \tag{3}$$

where α is the inclination of an element of the aerial wire with the horizontal plane and is constant. It is obvious that a and z can be made to vary with ϕ in any way.

The conical helix used by us for studying the charge distribution and the polar diagram of the radiation pattern was made of $\frac{5}{32}$-in. brass rod and had 10 turns. The radius at the base was 30 cm. The radius decreased uniformly to 10 cm at the apex in 10 turns within a height of 112 cm. A brass sheet, 100 cm in diameter, provided the "ground." Measurements were made with the helix oriented in two different ways with respect to the ground. First the base of the cone was close to the ground, and secondly the apex was close to the same. (The distance between the point closest to the ground and the ground was 1 cm in each case.) For each of these two cases polar diagrams were plotted, first, when the feed was at the base, and secondly, when the feed was at the apex. The feed arrangement for each of the cases is illustrated in Fig. 2.

Measurement of the Electric Field

The vertical and horizontal components of the electric field were measured with a small dipole placed at a

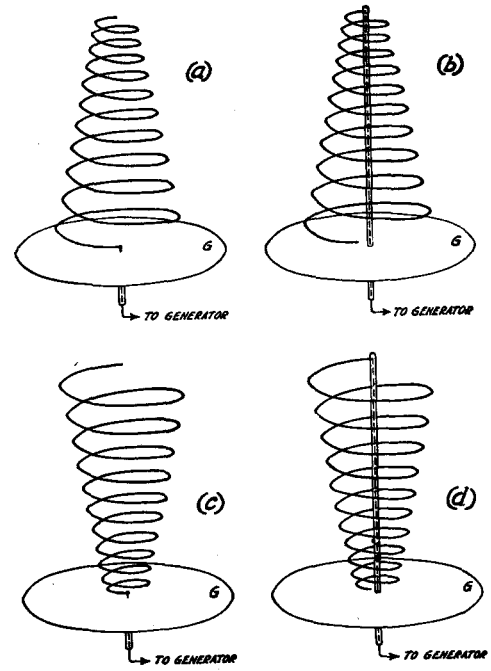

FIG. 2. Illustrating the different methods of feeding energy to the conical helix for different dispositions with respect to "ground." For case (a) the feed is at the base; (b) the feed is at the apex, the feeder passing axially through the helix; (c) feed at the apex; (d) feed is at the base, the feeder passing axially through the helix. Case (b) has the largest useful band width. For case (a) the band width is smaller, but the directivity is stronger.

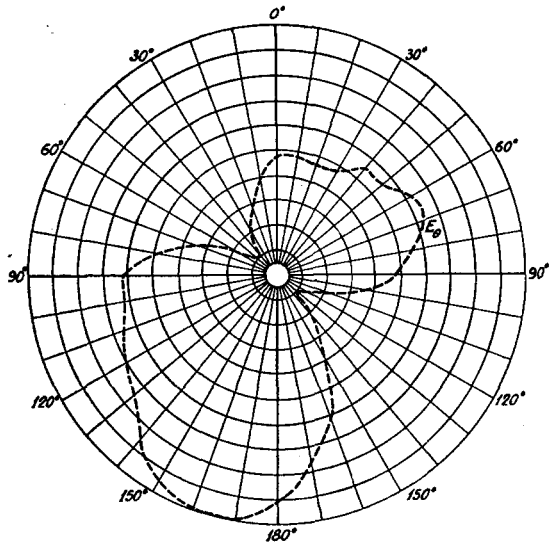

FIG. 3(a). E_θ radiation pattern of the conical helix shown in Fig. 2a. Base is close to the "ground." Energy feed is at the base. Frequency, 120 Mc/sec.

distant point and at the same height as the axis of the aerial. The polar diagrams as obtained for the four cases are shown in Figs. 3–6. The polar diagrams are necessarily different for the four cases because of the different current distributions.

Measurement of the Charge

The current distribution along the antenna can be found by measuring the voltage induced in a balanced loop placed in the axial slot in the aerial as had been done by Marsh.[3] This method, however, is not suitable here as the antenna wire is thin. The charge distribution was measured by coupling capacitatively a small probe to the antenna wire. The coupling was kept small so as not to distort the current distribution. The charge distributions for the top and the bottom feed for the normal and the inverted cone are shown in Figs. 7 and 8. For the case of the top feed, the charge distributions for 100 Mc/sec, 200 Mc/sec, and 300 Mc/sec were measured and for the bottom feed, charge distribution for 200 Mc/sec is shown.

In the case of a circular helix radiating in the axial mode, there are two modes of current propagation, namely, the T_0 and T_1 modes, both in the forward and in the reverse direction. The characteristic of the T_0 mode is that its phase velocity is equal to that of light when the diameter of helix D exceeds 0.5λ. For the T_0 mode, the current is rapidly attenuated and is of negligible amplitude within a few turns. The T_1 mode of current, however, is of constant amplitude along the helix and its phase velocity is smaller than that of light, being a function of pitch angle and of D/λ. The energy reaching the end of a helix of several turns is, thus, that produced by the T_1 mode of current.

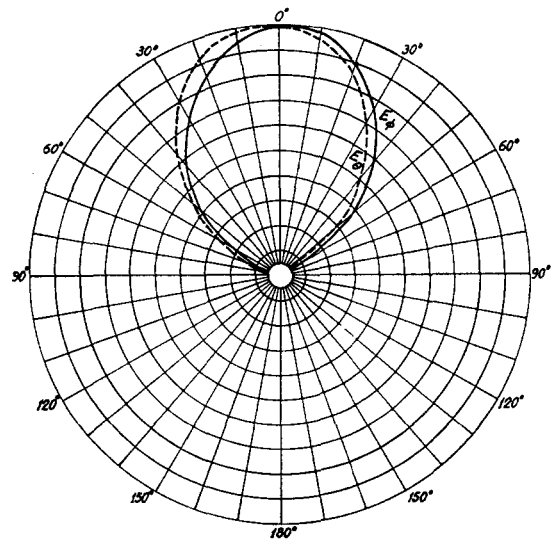

FIG. 3(b). E_ϕ and E_θ radiation patterns of the conical helix shown in Fig. 2a. Base is close to the "ground." Energy feed is at the base. Frequency, 150 Mc/sec.

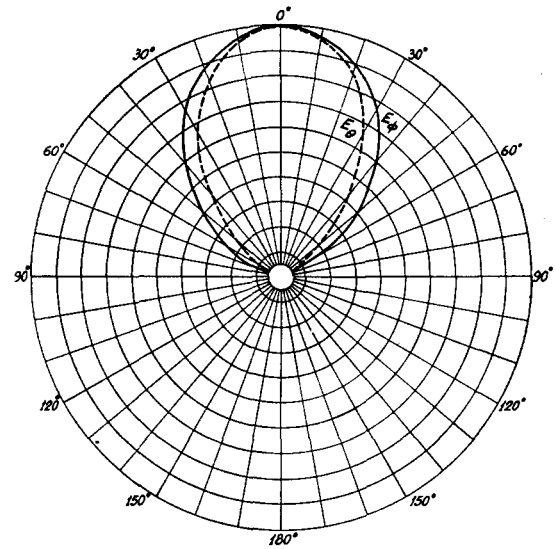

FIG. 3(c). E_ϕ and E_θ radiation patterns of the conical helix shown in Fig. 2a. Base is near the "ground." Feed is at the base. Frequency, 200 Mc/sec.

The current distribution along the length of the conical antenna is, however, much more complicated than that of the cylindrical helix. This is not only because there are several waves traveling with different propagation constants in both directions, but also because the propagation constants of the various modes of current cannot be assumed to be constant along the length of the aerial. In the absence of any theoretical analysis, the following qualitative information regarding the current distributions may be inferred from the experimentally obtained charge distribution. (a) From Fig. 7(a) it is seen that at 100 Mc/sec the T_0 mode is predominant, and pure standing waves are obtained. The propagation velocity is that of light. (b) Figure 7(b)

shows that at 200 Mc/sec the T_1 mode is excited, and the T_0 mode is attenuated. It is also seen that the current is almost zero at the base of the helix. This means that only progressive waves of current exist, and the charge and the current distributions are, therefore, identical. Further, the T_1 mode of current now grows in amplitude along the length of the aerial and is then attenuated. This is to be expected from the results of measurements by Marsh[3] on the circular helix, which indicates that the T_1 mode of current cannot be excited for all the values of D/λ. Since D varies continuously in the case of conical helix, the T_1 mode of current grows and after reaching a maximum amplitude is attenuated. It is also seen that the maximum amplitude of the current is obtained when $D=0.21\lambda$. (c) Figure 7(c) shows the charge distribution for 300 Mc/s. It is of the same nature as Fig. 7(b), except that the maximum

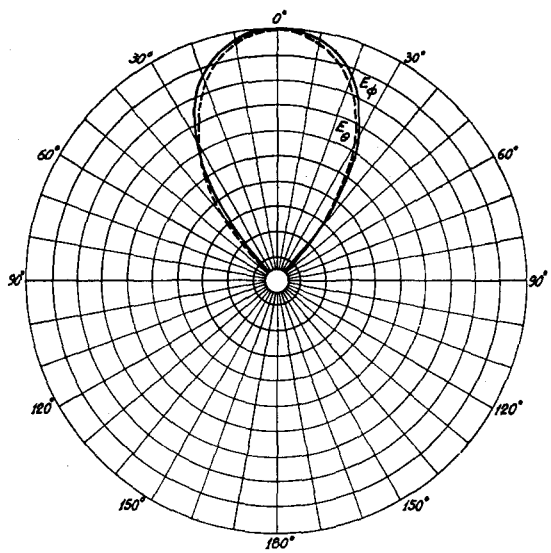

FIG. 3(d). E_ϕ and E_θ radiation patterns of the conical helix shown in Fig. 2a. Base is near the "ground." Feed is at the base. Frequency, 300 Mc/sec.

amplitude of the T_1 mode is now at the feed point of the helix when $D=0.2\lambda$.

One important feature of the current distribution is to be noted in each of the cases illustrated. The current distribution is almost zero in the region farther from the feed point, i.e., near the base, for all frequencies higher than that at which the axial mode of radiation appears. This means that the reflection coefficient is zero near the base, or, in other words, the antenna has a constant input impedance over this entire band of higher frequencies.

III. THEORETICAL ANALYSIS

We shall calculate the electric field for the T_1 mode of current distribution. This is because this mode causes the axial radiation which is of chief interest. For the circular helix the electric field at a distant point has

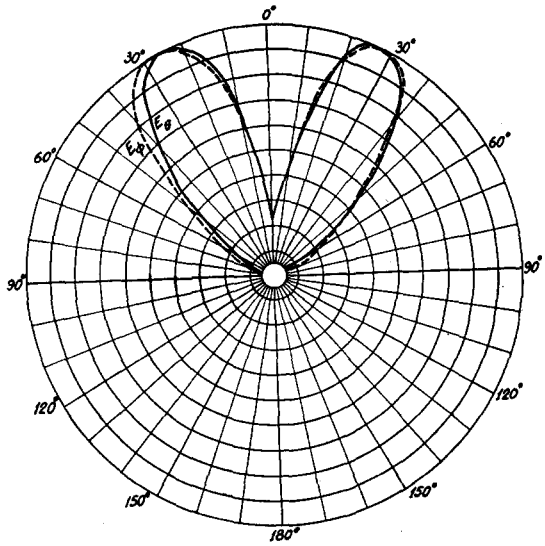

FIG. 3(e). E_ϕ and E_θ radiation patterns of the conical helix shown in Fig. 2a. Base is near the "ground." Feed is at the base. Frequency, 400 Mc/sec.

been calculated amongst others[2,4] by Kornhauser,[5] by determining the vector potential for the whole of the helix assuming a certain current distribution. Such a procedure is not suitable for the conical helix, because it leads to nonintegrable terms. Instead, the electric fields are calculated for the separate turns, and the total electric field is then obtained by combining them. This, of course, is possible if the distribution of phase velocity is known along the aerial.

The electric field E for the far zone is given by

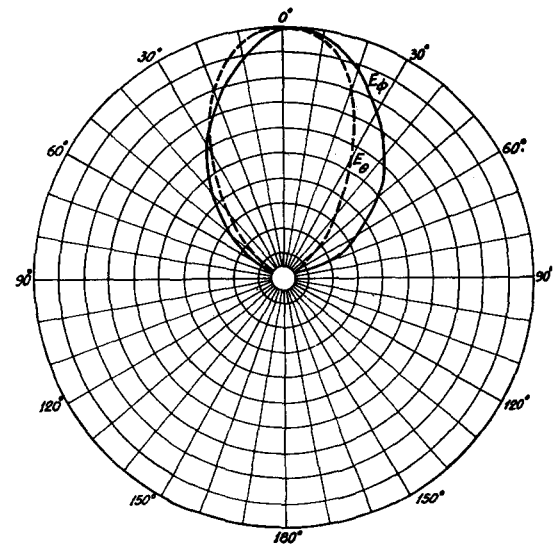

FIG. 4(a). E_ϕ and E_θ radiation patterns of the conical helix shown in Fig. 2b. Base is near the "ground." Feed is at the apex. Frequency, 150 Mc/sec.

[4] H. Lottrup Knudsen, Trans. Danish Acad. Tech. Sci., No. 8, pp. 55 (1950).
[5] E. T. Kornhauser, J. Appl. Phys. 22, 887 (1951).

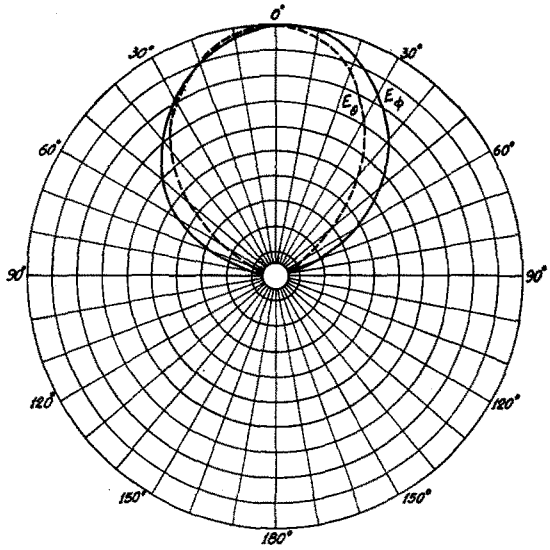

FIG. 4(b). E_ϕ and E_θ radiation patterns of the conical helix shown in Fig. 2b. Base is near the "ground." Feed is at the apex. Frequency, 200 Mc/sec.

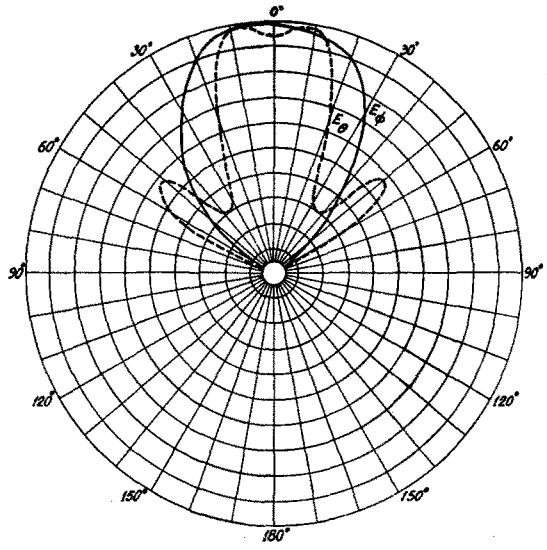

FIG. 4(d). E_ϕ and E_θ radiation patterns of the conical helix shown in Fig. 2b. Base is near the "ground." Feed is at the apex. Frequency, 450 Mc/sec.

(King[6])

$$E=\frac{j\omega\mu_0}{4\pi R}\int\{\mathbf{R}_0\times(\mathbf{R}_0\times\mathbf{S})\}I\cdot\exp(-j\beta_0 R)\cdot ds, \quad (4)$$

where ω is the angular frequency, μ_0 is the absolute permeability of space. R is the distance between the point at which the electric field is calculated and ds, the element of the aerial wire carrying the current I. $\mathbf{R}_0$ is the unit radial vector in a spherical coordinate system (r, θ, ϕ) with the aerial at the origin. $\mathbf{S}$ is the unit vector along the antenna and thus varies in direction along the aerial.

The vector product

$$\{\mathbf{R}_0\times(\mathbf{R}_0\times\mathbf{S})\}=S_\theta\cdot\boldsymbol{\theta}-S_\phi\cdot\boldsymbol{\phi}, \quad (5)$$

where S_θ and S_ϕ are the direction cosines between $\mathbf{S}$ and the θ, ϕ spherical coordinate axes, and are given by

$$S_\theta=-\cos\alpha\cdot\cos\theta\left\{\sin\phi-\frac{k_m\cos\phi}{1-k_m\phi}\right\}-\sin\alpha\cdot\sin\theta,$$

$$S_\phi=\cos\alpha\left\{\cos\phi-\frac{k_m\sin\phi}{1-k_m\phi}\right\}. \quad (6)$$

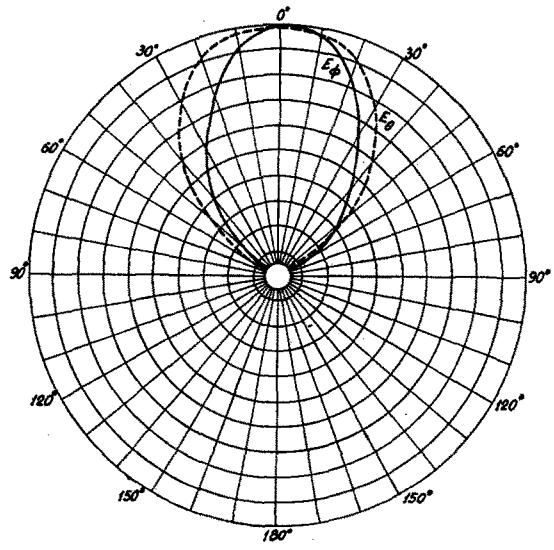

FIG. 4(c). E_ϕ and E_θ radiation patterns of the conical helix shown in Fig. 2b. Base is near the "ground." Feed is at the apex. Frequency, 300 Mc/sec.

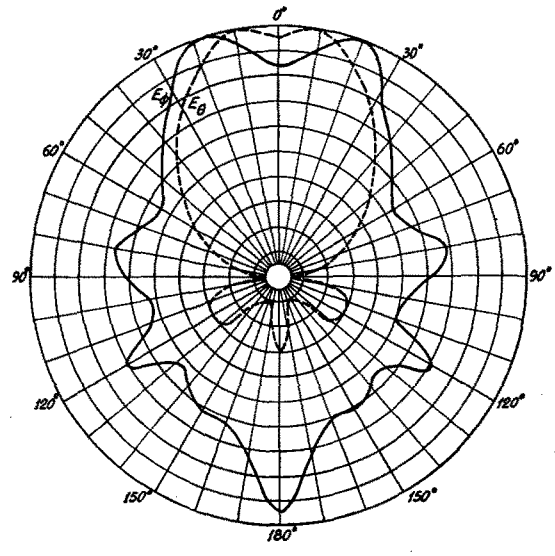

FIG. 5(a). E_ϕ and E_θ radiation patterns of the conical helix with the apex close to the "ground." Feed is at the base. Frequency, 150 Mc/sec.

[6] R. W. P. King, *Electromagnetic Engineering* (McGraw-Hill Book Company, Inc., New York, 1945), Vol. 1, pp. 271.

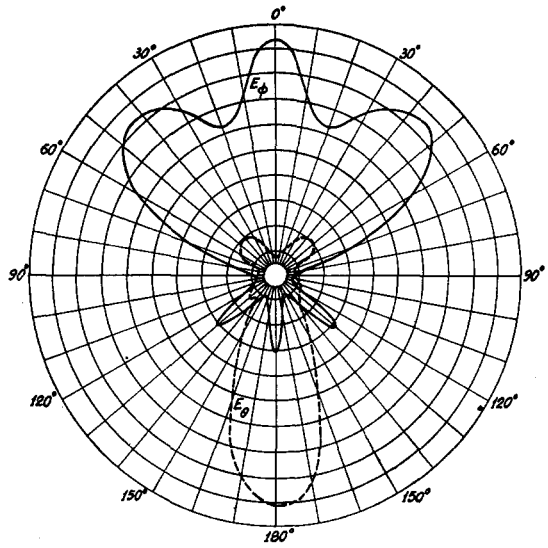

FIG. 5(b). E_ϕ and E_θ radiation patterns of the conical helix with the apex close to the "ground." Feed is at the base. Frequency, 200 Mc/sec.

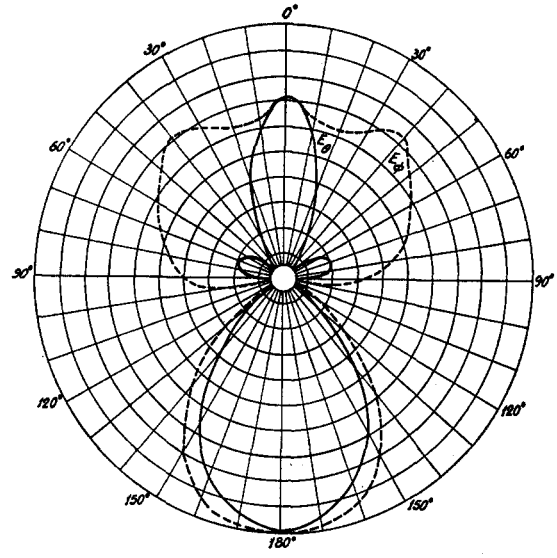

FIG. 6(a). E_ϕ and E_θ radiation patterns of the conical helix. Apex is close to the "ground" and feed is at the apex. Frequency, 150 Mc/sec.

The ϕ-axis of the spherical coordinate system is taken in the same plane as that of the cylindrical coordinate systems.

From the helix geometry

$$s = a_m \sec\alpha \cdot \phi(1 - k_m\phi/2), \tag{7}$$

$$ds = a_m \sec\alpha \cdot (1 - k_m\phi) \cdot d\phi. \tag{8}$$

Since R is large compared to the dimensions of the helix, it is replaced except in the phase term by R_0, the distance between the origin of the coordinate system and the distant point at which electric field is to be calculated. This approximation cannot obviously be made for the phase term. The value of R for the mth loop is given by (Fig. 9)

$$\begin{aligned} R_m &= R_0 - (z_m + z)\cos\theta - a_m(1 - k_m\phi)\sin\theta \cdot \cos\phi \\ &= R_0 - z_m\cos\theta - a_m \tan\alpha \cdot \phi \cdot \cos\theta \\ &\quad + a_m \tan\alpha \cdot \cos\theta \cdot k_m\phi^2/2 - a_m \sin\theta \cdot \cos\phi \\ &\quad + a_m k_m \sin\theta \cdot \phi \cdot \cos\phi, \end{aligned} \tag{9}$$

where z_m and a_m are values of z and a, respectively, at the center of mth loop. k_m is the value of k for the mth loop.

Since the T_1 mode of current attenuates slowly, it is assumed for simplicity of calculation that the current remains constant over one turn and varies from turn

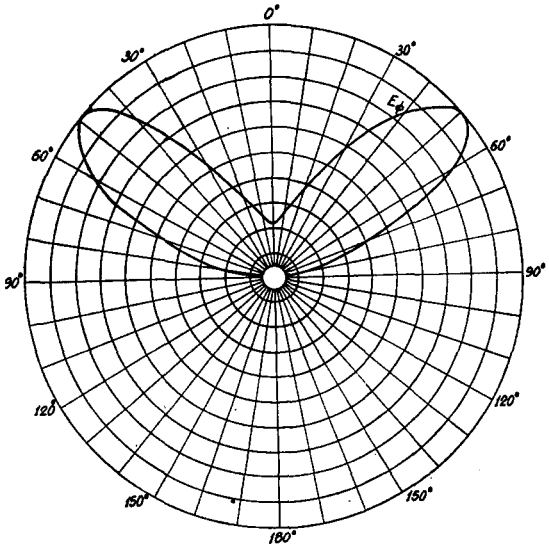

FIG. 5(c). E_ϕ radiation pattern of the conical helix with the apex close to the "ground." Feed is at the base. Frequency, 300 Mc/sec.

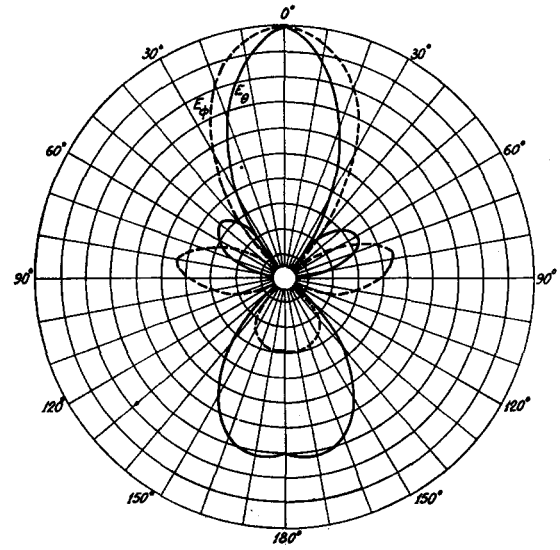

FIG. 6(b). E_ϕ and E_θ radiation patterns of the conical helix. Apex is close to the "ground" and feed is at the apex. Frequency, 200 Mc/sec.

to turn by appropriate amounts. A linear variation of phase velocity is assumed. Thus the current I in the mth loop, referred to the phase of the current in the first loop is given by

$$I = I_m \exp(-j\nu_m)\cdot\exp(-j\omega s/v), \tag{10}$$

where ν_m = phase difference between the current at the centers of first loop and mth loop, and v is the phase velocity and is given by

$$\begin{aligned} v &= v_m(1-h_m\phi) \\ &\doteq v_m/(1+h_m\phi), \end{aligned} \tag{11}$$

since the maximum value of ϕ is π and h_m is small. Substituting Eqs. (6)–(11) in Eq. (5), E_ϕ and E_θ are obtained. Thus,

$$\begin{aligned} E_\phi = -\frac{j\omega\mu_0}{4\pi R_0}\sum_{m=1}^{N}\int_{-\pi}^{+\pi}\Bigg[&\cos\alpha\left\{\cos\phi-\frac{k_m\sin\phi}{1-k_m\phi}\right\} \\ &\times\exp\left(-\overset{\omega}{j}R_m\right)\cdot I_m\cdot\exp(-j\nu_m) \\ &\times\exp\left\{-j\frac{\omega a_m\sec\alpha}{v_m}\left(\phi-\frac{k_m\phi^2}{2}\right)(1+h_m\phi^2)\right\} \\ &\times a_m\sec\alpha(1-k_m\phi)\Bigg]d\phi, \end{aligned} \tag{12}$$

where N is the number of turns.

Substituting the value of R_m from Eq. (9),

$$\begin{aligned} E_\phi = -\frac{j\omega\mu_0\exp(-j\omega R_0/c)}{4\pi R_0}\sum_{m=1}^{m=N} a_m I_m \\ \times\exp\left(\overset{\omega}{j}z_m\cos\theta-j\nu_m\right) \\ \times\int_{-\pi}^{+\pi}\Bigg[\{\cos\phi(1-k_m\phi)-k_m\sin\phi\} \\ \times\exp\left(\overset{\omega}{j}a_m\tan\alpha\cdot\cos\theta\cdot\phi-\overset{\omega}{j}a_m\tan\alpha\right. \\ \left.\times\cos\theta\cdot\frac{k_m}{2}\phi^2+\overset{\omega}{j}a_m\sin\theta\cdot\cos\phi\right) \\ \times\exp\left(-\overset{\omega}{j}a_m k_m\sin\theta\cdot\phi\cdot\cos\phi\right) \\ \times\exp\left\{-\frac{j\omega a_m\sec\alpha\cdot\phi}{v_m}-\frac{j\omega a_m\sec\alpha}{v_m}\right. \\ \left.\times(h_m-k_m/2)\phi^2+\frac{j\omega a_m h_m k_m}{2v_m}\cdot\phi^3\right\}\Bigg]d\phi. \end{aligned} \tag{13}$$

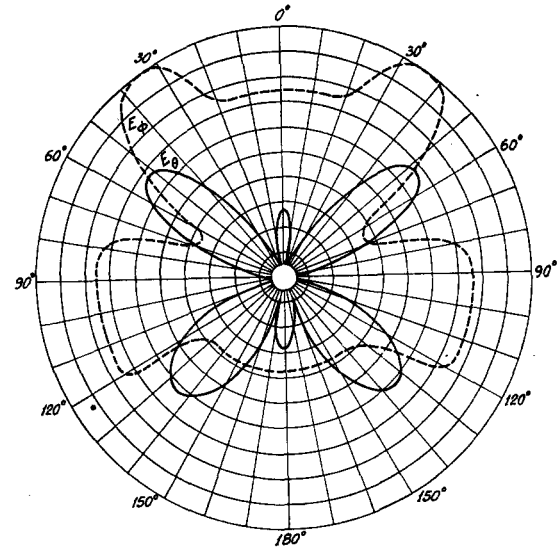

FIG. 6(c). E_ϕ and E_θ radiation patterns of the conical helix. Apex is close to the "ground" and feed is at the apex. Frequency, 300 Mc/sec.

Or, with the abbreviations,

$$E_0 = -\frac{j\omega\mu_0\exp(-j\omega R_0/c)}{4\pi R_0},$$

$$n_{\theta m} = \overset{\omega}{-}z_m\cdot\cos\theta,$$

$$\psi_{\theta m} = n_{\theta m} - \nu_m,$$

$$\mathfrak{C}_{\theta m} = \overset{\omega}{-}a_m\tan\alpha\cdot\cos\theta,$$

$$d_{\theta m} = \overset{\omega}{-}a_m\sin\theta,$$

$$g_m = \overset{\omega}{-}a_m\sec\alpha. \tag{14}$$

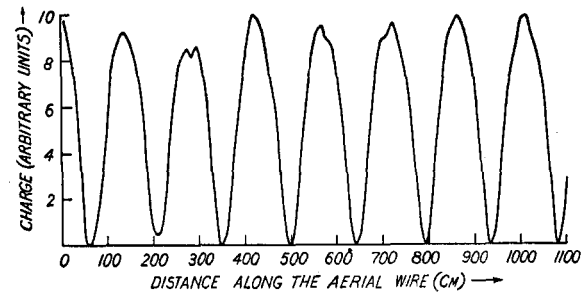

FIG. 7(a). Charge distribution along the length of the conical helix shown in Fig. 2. Base is close to the "ground" and feed is at the apex. Excitation frequency, 100 Mc/sec.

Equation (13) can be written as

$$E_\phi = E_0 \sum_{m=1}^{N} a_m I_m \exp(j\psi_{\theta m}) \int_{-\pi}^{+\pi} \times \Big[\{\cos\phi(1-k_m\phi) - k_m \sin\phi\} \exp j(\mathfrak{C}_{\theta m} - g_m)\phi \times \exp -j\{g_m(h_m - k_m/2) + \mathfrak{C}_{\theta m} \cdot k_m/2\}\phi^2 \times \exp\left(-jg_m h_m \frac{k_m}{2} \cdot \phi^3\right) \times \exp(jd_\theta \cos\phi) \cdot \exp(-jd_\theta k_m \phi \cdot \cos\phi) \Big] d\phi. \quad (15)$$

The right-hand side of the equation cannot in general be integrated. In the particular case where k_m is small, which is of importance, the expression can be simplified. Since the maximum value of ϕ is π, and $g_m h_m k_m \pi^3/2 \ll 1$, we can put,

$$\exp(-jg_m h_m(\tfrac{1}{2}k_m) \cdot \phi^3) \doteqdot 1,$$

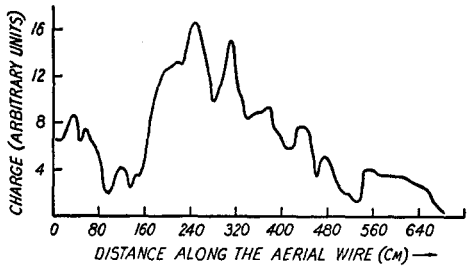

FIG. 7(b). Charge distribution along the length of the conical helix shown in Fig. 2. Base is close to the "ground" and feed is at the apex. Excitation frequency, 200 Mc/sec.

and

$$\exp(-jd_\theta k_m \phi \cos\phi) \doteqdot 1 - jd_\theta k_m \phi \cos\phi \doteqdot 1.$$

Writing,

$$g_m(h_m - k_m/2) + \mathfrak{C}_{\theta m} k_m/2 = H \quad (16)$$

and using the Fourier expansion for $\exp(jd_\theta \cos\phi)$, i.e.,

$$\exp(jd_\theta \cos\phi) = \sum_{n=-\infty}^{n=+\infty} j^n J_n(d_\theta) \exp(jn\phi), \quad (17)$$

where $J_n(d_\theta)$ is the nth order Bessel function for the argument d_θ. Eq. (15) can be written as

$$E_\phi = E_0 \sum_{m=1}^{N} a_m I_m \exp(j\psi_{\theta m}) \int_{-\pi}^{+\pi} \times \Big[\{\cos\phi(1-k_m\phi) - k_m \sin\phi\} \exp\{j(v_{\theta m} - g_m)\phi\} \times (1 - jH\phi^2) \times \sum_{n=-\infty}^{n=+\infty} j^n J_n(d_\theta) \exp(jn\phi) \Big] d\phi.$$

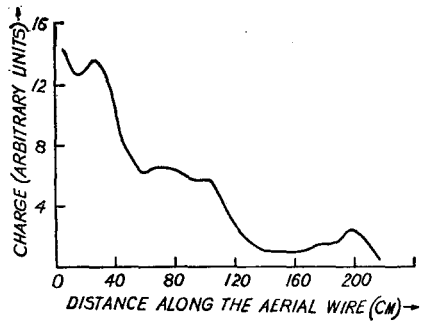

FIG. 7(c). Charge distribution along the length of the conical helix shown in Fig. 2. Base is close to the "ground" and feed is at the apex. Excitation frequency, 300 Mc/sec.

Or, rearranging the terms,

$$E_\phi = E_0 \sum_{m=1}^{N} a_m I_m \exp(j\psi_{\theta m}) \sum_{n=-\infty}^{n=+\infty} j^n J_n(d_\theta) \times \int_{-\pi}^{+\pi} \Big[\{\cos\phi(1-k_m\phi) - k_m \sin\phi\} \times (1 - jH\phi^2) \exp\{j(\mathfrak{C}_{\theta m} - g_m + n)\phi\} \Big] d\phi. \quad (18)$$

Introducing the exponential forms of $\cos\phi$ and $\sin\phi$ and putting,

$$\left.\begin{aligned} x &= v_{\theta m} - g_m + n + 1 \\ y &= v_{\theta m} - g_m + n - 1 \end{aligned}\right\}, \quad (19)$$

and also neglecting second-order terms,

$$E_\phi = \frac{E_0}{2} \sum_{m=1}^{N} a_m I_m \exp(j\psi_{\theta m}) \sum_{n=-\infty}^{n=+\infty} j^n J_n(d_\theta) \times \int_{-\pi}^{+\pi} \Big[(1 + jk_m - k_m\phi - jH\phi^2) \exp(jx\phi) + (1 - jk_m - k_m\phi - jH\phi^2) \exp(jy\phi) \Big] d\phi \quad (20)$$

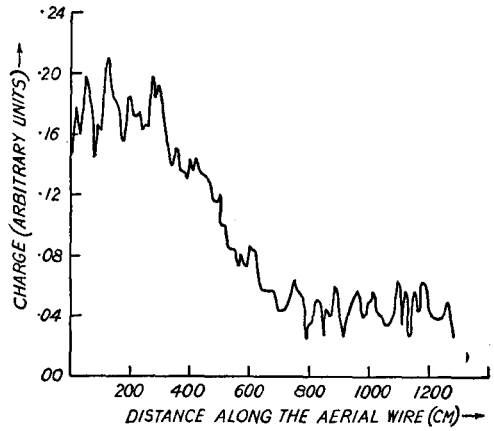

FIG. 8. Charge distribution along the length of the conical helix shown in Fig. 2. Base is close to the "ground" and feed is at the base. Excitation frequency, 200 Mc/sec.

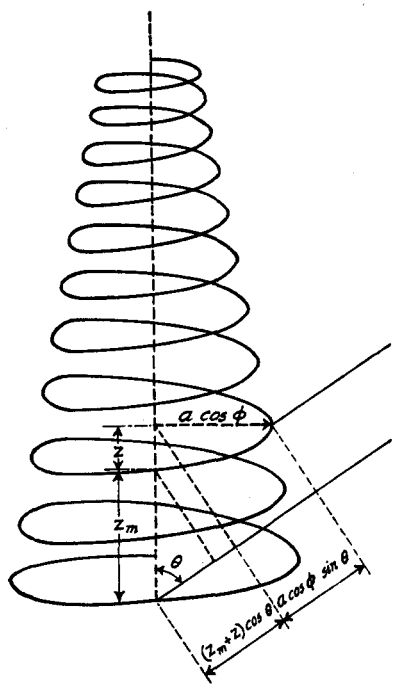

FIG. 9. Illustrating the calculation of the distance, from a point in the far zone, of an element ds of a loop of the helix with reference to the distance of the same point from the origin.

$$= E_0 \sum_{m=1}^{N} a_m I_m \exp(j\psi_{\theta m}) \sum_{n=-\infty}^{n=+\infty} j^n J_n(d_\theta)$$

$$\times\Bigg[\Bigg\{(1+jk_m)\frac{\sin x\pi}{x} - k_m\left(-j\pi\frac{\cos x\pi}{x} + j\frac{\sin x\pi}{x^2}\right)$$

$$-jH\left(\pi^2\frac{\sin x\pi}{x} + 2\pi\frac{\cos x\pi}{x^2} - \frac{2\sin x\pi}{x^3}\right)\Bigg\}$$

$$+\Bigg\{(1-jk_m)\frac{\sin y\pi}{y} - k_m\left(-j\pi\frac{\cos y\pi}{y} + j\frac{\sin y\pi}{y^2}\right)$$

$$-jH\left(\pi^2\frac{\sin y\pi}{y} + 2\pi\frac{\cos y\pi}{y^2} - \frac{2\sin y\pi}{y^3}\right)\Bigg\}\Bigg]. \quad (21)$$

We next obtain the θ-component of the electric field at the distant point. Substituting Eq. (7) in Eq. (5), E_θ is given by

$$E_\theta = -\frac{j\omega\mu_0}{4\pi R_0}\sum_{m=1}^{N}\int_{-\pi}^{+\pi}\Bigg[\cos\alpha\Bigg\{\cos\theta\left(\sin\phi - \frac{k_m\sin\phi}{1-k_m\phi}\right)$$

$$+\tan\alpha\cdot\sin\theta\Bigg\}\cdot\exp\left(-j\frac{\omega}{c}R_m\right)\cdot I_m\exp(-jv_m)$$

$$\times\exp\left\{j\frac{\omega a_m\sec\alpha}{v_m}\left(\phi - \frac{k_m\phi^2}{2}\right)(1+h_m\phi^2)\right\}$$

$$\times a_m\sec\alpha(1-k_m\phi)\Bigg]d\phi. \quad (22)$$

Proceeding as before this expression can be simplified and E_θ is given by,

$$E_\theta = E_0\sum_{m=1}^{N} a_m I_m\exp(j\psi_{\theta m})\sum_{n=-\infty}^{n=+\infty} j^n J_n(d_\theta)$$

$$\times\Bigg[j\cos\theta\Bigg\{(jk_m-1)\frac{\sin x\pi}{x}$$

$$+k_m\left(-j\pi\frac{\cos x\pi}{x} + j\frac{\sin x\pi}{x^3}\right)$$

$$+jH\left(\pi^2\frac{\sin x\pi}{x} + 2\pi\frac{\cos x\pi}{x^2} - \frac{2\sin x\pi}{x^3}\right)$$

$$+(1+jk_m)\frac{\sin y\pi}{y} - k_m\left(-j\pi\frac{\cos y\pi}{y} + j\frac{\sin y\pi}{y^2}\right)$$

$$-jH\left(\pi^2\frac{\sin y\pi}{y} + 2\pi\frac{\cos y\pi}{y^2} - \frac{2\sin y\pi}{y^3}\right)\Bigg\}$$

$$+2\tan\alpha\sin\theta\Bigg\{\frac{\sin u\phi}{u} - k_m\left(-j\pi\frac{\cos u\pi}{u} + j\frac{\sin u\pi}{u^2}\right)$$

$$-jH\left(\pi^2\frac{\sin u\pi}{u} + 2\pi\frac{\cos u\pi}{u^2} - \frac{2\sin u\pi}{u^3}\right)\Bigg\}\Bigg], \quad (23)$$

where $u = \mathfrak{C}_{\theta m} - g_m + n$.

The expressions for E_ϕ and E_θ are long, but some of the terms are quite small compared with the others. In the series

$$\sum_{n=-\infty}^{n=+\infty} j^n J_n(d_\theta),$$

the zeroth term is the largest and all others, except $n=\pm 1$, can be neglected as they are less than 1 percent. Of the terms in the parenthesis, $\sin x\pi/x$, $\sin y\pi/y$, $\sin u\pi/u$ are by far the largest terms and of these $\sin x\pi/x$ term is very large.

In Fig. 10 the experimental and theoretical polar diagrams for a conical helix (base nearer the ground), fed at base, are compared for 200 Mc/sec excitation.

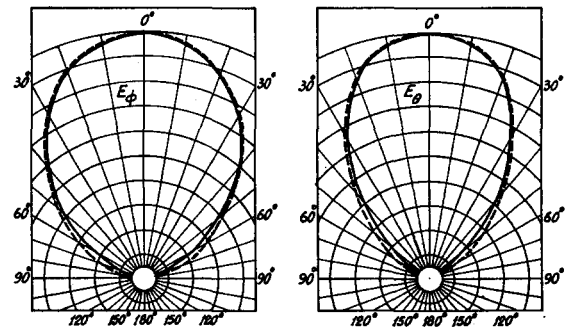

FIG. 10. Calculated (dotted lines) and observed (solid lines). E_ϕ and E_θ radiation patterns for the case shown in Fig. 3(c).

Only the first-order terms have been retained in the calculation. The phase velocity has been obtained from the following relation as used by Kraus:[7]

$$L/p=\lambda+(\lambda/2N)+Z, \qquad (24)$$

where $p=v/c$, $L=$length of one turn, $Z=$the distance between the turns for the conical helix. The actual phase velocity for the conical helix may be slightly different from that given by Eq. (24) because all the turns are not of same diameter.

IV. CONCLUDING REMARKS

We note that while in a circular helix the axial mode of radiation can be maintained over a frequency range of about one octave, that in a conical helix can be maintained over a much wider frequency range by suitably varying the diameter. For a wide band conical helix the axial mode of radiation is, however, likely to be mixed with the normal mode in the low side of the frequency band. The relative magnitudes of the axial and the normal radiations depend on the pitch angle, the degree of tapering, and also on the feed position.

The conical helix can be modified in several ways for special applications. Some of these variations are shown in Fig. 11.

In Fig. 11(a) a conical helix in which the radius is constant in the central part is shown. This will have a sharper radiation pattern in the middle of the frequency band over which it can be used. The conical helix as shown in Fig. 11(b) is suited for balanced feeder. If the pitch angle is zero the conical helix reduces to a spiral as shown in Fig. 11(d). With appropriate delays at suitable intervals along the length as shown in Fig. 11(e), the spiral will radiate most of the energy in a direction perpendicular to the plane for a wide frequency range. Figure 11(e) shows a combination of spiral and conical helix which will have large band width with small height of the aerial above the ground.

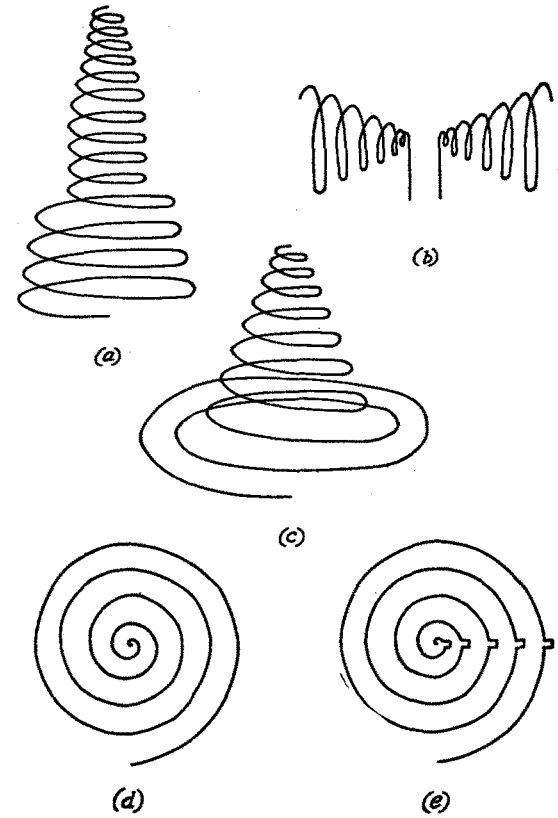

FIG. 11. Some modifications of the conical helix.

This type of aerial may be useful for ionospheric investigations.

ACKNOWLEDGMENT

The above investigations were carried out in the Institute of Radio Physics and Electronics, Calcutta University. The author wishes to express his sincere gratitude to Professor S. K. Mitra for constant encouragement and helpful advice during the progress of the work.

[7] J. D. Kraus, Proc. Inst. Radio Engrs. 37, 263 (1949).